IOP Publishing | Measurement Science and Technology

Meas. Sci. Technol. 31 (2020) 055106 (14pp) https://doi.org/10.1088/1361-6501/ab6917

Accurate foot clearance estimation during level and uneven ground walking using inertial sensors

Bingfei Fan[1], **Qingguo Li**[2] and **Tao Liu**[1]

[1] State Key Laboratory of Fluid Power and Mechatronic Systems, School of Mechanical Engineering, Zhejiang University, Hangzhou 310027, People's Republic of China

[2] Department of Mechanical and Materials Engineering, Queen's University, Kingston, ON K7L 3N6, Canada

E-mail: liutao@zju.edu.cn

Received 16 May 2019, revised 23 December 2019
Accepted for publication 8 January 2020
Published 5 March 2020

Abstract

Foot clearance during walking is considered as a key indicator for assessing fall risk, obstacle negotiation strategies and energy expenditure. Foot clearance estimation using inertial measurement units (IMUs) has the advantages of small size, low cost and user-friendliness. However, its application is still limited due to issues with accuracy and reliability. In this paper, we aimed at understanding the limiting factors in foot clearance estimation using low-cost IMUs and proposed a foot clearance estimation method with millimeter-level accuracy. We first analyzed each component in conventional double-integration-based foot clearance estimation, and then proposed a set of new procedures for foot trajectory estimation, including a gait-adaptive complementary filter for orientation estimation, a two-IMU configuration and a shock absorber. Finally, we extracted the foot clearance from the estimated foot trajectory. In the experiments, we recruited eight healthy subjects and instructed them to walk under level and uneven ground conditions; moreover, to validate the applicability of the proposed method, we also instructed the subjects to mimic pathological gaits, including ataxic gait (zigzag walking), waddling gait and Parkinsonian gait. A total of 2640 gait cycles were collected and the extracted foot clearances were benchmarked with the optical motion capture system. With the proposed method, the average mean and standard deviation of the extracted maximal heel clearance and minimal toe clearance in all the gait cycles were -0.34 ± 0.24 cm and 0.02 ± 0.26 cm. The results are more accurate than in previous studies. Most importantly, the proposed method does not require any post correction and flat-floor assumption. The presented foot clearance estimation method provides an applicable and practical clinical solution not only for heel and toe clearance estimation but also for foot trajectory estimation.

Keywords: foot clearance, foot trajectory, inertial sensors, orientation estimation, fall risk assessment

(Some figures may appear in colour only in the online journal)

1. Introduction

Gait analysis is considered to be an effective way of assessing human mobility [1]. The temporal and spatial gait parameters obtained from gait analysis can be used to characterize changes of gait in the elderly and people with mobility disorders such as cerebellar ataxia, myopathy and Parkinson's disease [2, 3]. Among these gait parameters, the foot clearance, which refers to the distance between the foot and the ground, is considered to be an important indicator for risk of fall. Insufficient foot clearance will increase the risk of tripping in forward walking [4, 5], and quantification of fall risk is essential for fall prevention and intervention [6, 7]. Foot clearance is also related to energy expenditure as well as safety during obstacle-crossing [8], and it is also a safety indicator when going up and down stairs [9]. Accurate foot clearance estimation is significant in these applications.

The conventional foot clearance measurement system is the optical motion capture system, which uses multiple cameras to track the positions of reflective markers located on shoes, and then determines heel and toe clearance [10, 11]. This method is accurate and reliable and is often regarded as the gold standard in foot clearance estimation. However, this method has a variety of shortcomings. It is inevitably expensive and can only track a limited number of steps within a laboratory setting. Hence, it cannot be used as a convenient means to analyze the natural gait in the daily living environment.

Wearable sensors are becoming more and more accurate, with a small size, and low cost. Microelectromechanical systems (MEMS)-based inertial measurement units (IMUs) have been shown to be an attractive solution for ambulatory estimation of foot clearance [12]. The IMUs can be easily attached to shoes for continuous outdoor gait tracking without disturbing natural gaits. Foot clearance is the vertical component of foot displacement, which can be estimated by double integration of the foot acceleration in the earth frame [13–15]. In this estimation process, the error in sensor orientation estimation and accumulative errors from double integration will inevitably lead to large errors in displacement estimations. In a broader sense, displacement-related gait parameters include stride length, foot clearance, step width, etc. A large number of studies focus on the displacement in the horizontal plane such as stride length, walk distance, etc, and the stride length estimation has achieved very good accuracy with total distance estimation error as small as 1% [16]. However, in the vertical direction, the foot clearance error is usually several centimeters [13, 17]. As the total height of toe clearance is only about 8–15 cm [18], the estimation error will cause a large relative percentage error. To date, foot clearance estimation with millimeter-level accuracy is still challenging.

IMU-based foot clearance estimations can be divided into two categories: the indirect and direct estimation methods. The indirect methods estimate the clearance of IMU first, and then calculate the heel and toe clearance through geometric transformations. In [13], Mariani *et al* proposed an IMU-based foot clearance estimation method. The IMU was mounted at the instep of the shoe. The algorithm calculated the displacement of the IMU and automatically estimated the location of the IMU, and then calculated the toe and heel clearance using geometric transformations. The reported accuracy of the maximum heel clearance (MaxHC) was 4.1 $\pm$ 2.3 cm (mean $\pm$ SD), and the minimal toe clearance (MinTC) was 1.3 $\pm$ 0.9 cm. The system was easy to wear and to use and provided a useful tool for gait analysis. In [19], Kanzler *et al* proposed a similar indirect foot clearance estimation method, where the IMU was placed at the heel of the shoe. The achieved accuracy was equivalent to the accuracy in [13]. Both of the studies were based on the assumption of level ground walking, which made the presented methods only suitable in level ground walking. The achieved centimeter-level accuracy was not enough, especially when analyzing the toe clearance variability, because the observed MinTC variability during walking was only about several millimeters [20]. The advantages of the indirect methods are that only one IMU is required and the placement of IMU is not restricted. However, in the indirect calculation process, errors in the IMU location estimation and the relative motion of IMU will increase the error of foot clearance estimation.

Another category is direct foot clearance estimate methods [17, 21, 22]. In these methods, the IMU is placed near the toe or heel, so that the estimated clearance of the IMU can be regarded as the toe or heel clearance. In [17], Hannink *et al* measured the heel clearance by placing an IMU beside the heel; several typical combinations of the orientation estimation method and double-integration schemes for displacement estimation were analyzed. The reported accuracy of the preferable combination was 1.97 $\pm$ 3.56 cm. In [14], Kitagawa and Ogihara developed a system to monitor foot clearance using an IMU placed at the instep. The mean accuracy and precision was approximately 0.2 $\pm$ 0.7 cm for foot clearance, which was much more accurate than previous studies [13]. However, this direct method relied on displacement correction based on the flat floor assumption, and the estimated clearance was the clearance of instep IMUs rather than the biomechanical toe and heel clearance.

Besides IMUs, miniature range sensors have also been used to measure the distance and these do not suffer from accumulative error. Several studies have attempted to combine range sensors with IMUs to get higher accuracy in foot clearance estimation [18, 23, 24]. Arami *et al* estimated the foot clearance by adding range sensors [18]. The authors compared the schemes of different combinations of range sensors and IMUs, and they concluded that the integration of the range sensor and IMU performed the best. The foot clearance estimation accuracy was 0.31 $\pm$ 0.93 cm. Although the accuracy had been improved by adding range sensors, it increased the system's complexity, and it also relied on the flat floor assumption. Moreover, the accuracy of the range sensor was influenced by floor materials and the foot angle between the shoe and ground. These limitations made range sensor-based systems less practical.

Since foot clearance estimation relies on accurate orientation estimation and double integration of acceleration, we believe that with the development of MEMS technologies and sensor fusion algorithms, the foot clearance accuracy can be improved without adding other types of sensors. Therefore, in this paper, we focused on developing an accurate foot clearance measurement system using only IMUs. We first systematically analyzed the key factors that influenced the accuracy of foot clearance estimation, including the accuracy of orientation estimation, sensor placement and shock absorption. Then, we proposed improved solutions for each component to achieve a reliable toe and heel clearance estimation with millimeter-level accuracy. Finally, to validate the applicability of the proposed method, we performed the experiments under various walking conditions, including not only level ground walking conditions, but also uneven ground walking and imitative pathological walking conditions.

2. Methods

2.1. Measurement system

An overview of the developed multiple-IMU system is shown in figure 1. This system was a redundant IMU system including three IMUs, where the instep IMU was used for the comparison study. Precisely, the instep IMU was placed flat at the instep. The heel IMU was first mounted on one end of a plastic sheet, and a shock absorber was used to attenuate the acceleration at heel strike. Then, the other end of the shock absorber was fixed on the side of the shoe sole, keeping the IMU close to the heel. Thus, the trajectory of the heel IMU represented the heel trajectory. The placement of the toe IMU was similar to the heel IMU. Although the physical coordinates of the three sensors were different, for convenience, we converted them to consistent coordinates where the Z axis pointed up, the X axis pointed left and the Y axis pointed back, as shown in figure 1. For the comparison study, we developed four estimators with different IMU configurations to estimate the foot clearance. The details of each estimator are listed in table 1. The instep IMU, toe IMU and heel IMU estimators are indirect methods using only one IMU, while the two-IMU estimator is a direct method using two independent IMUs. The two-IMU configuration is an improved configuration presented in this paper, and the others are the commonly used configurations in the literature.

The IMUs in this system were used to estimate the sensor trajectory, and the method of double integration of the acceleration was considered [17]. The overall schematic of the three-dimensional (3D) sensor trajectory calculation is shown in figure 2. The procedure includes sensor calibration, orientation estimation, gravity acceleration removal and double integration of the acceleration. In this paper, we focus on improving the key components in this procedure. The details of the improved solutions for each component are described in the following subsections.

2.2. Sensor orientation estimation

2.2.1. Basic sensor fusion algorithm. In figure 2, ${}^E_S q$ is the orientation quaternion of the sensor frame relative to the earth frame, which is estimated by fusing the accelerometer and gyroscope data. The accuracy of the orientation estimation determines the accuracy of motion acceleration after removing the gravity acceleration, and then affects the accuracy of the final displacement estimation. Therefore, accurate orientation estimation is extremely important. The challenge of accurate orientation estimation comes from the influence of the large acceleration during walking, which reaches up to 8–10 g sometimes [25]. To reduce the influence of the large acceleration, we adopt the state machine-based complementary filter presented in our previous study [25]. Only step one in the sensor fusion method is required because foot clearance estimation does not need heading information, thus it does not need a magnetometer. The implementation of the algorithm is described as follows.

Supposing that the orientation of the previous iteration is ${}^S_E\hat{q} = [q_0 q_1 \;\; q_2 q_3]$, the measured angular velocity in the sensor frame is ${}^S\omega = \begin{bmatrix}\omega_x & \omega_y & \omega_z\end{bmatrix}$. $\mathrm{A}({}^S_E\hat{q})$ is the rotation matrix representation of ${}^S_E\hat{q}$, and the measured acceleration is ${}^S a = \begin{bmatrix}a_x & a_y & a_z\end{bmatrix}$. The gravity acceleration is $g = \begin{bmatrix}0 & 0 & 1\end{bmatrix}$. Then, the predicted acceleration, a_p, can be calculated as

$$a_p = \mathrm{A}\left({}^S_E\hat{q}\right) \cdot g = \begin{bmatrix} 2q_1q_3 - 2q_0q_2 \\ 2q_2q_3 + 2q_0q_1 \\ 2{q_0}^2 - 1 + 2{q_3}^2 \end{bmatrix}. \qquad (1)$$

The difference, e_a, between the measured acceleration, $\hat{a}$, and the predicted acceleration, a_p, is calculated as the cross-product of them, as described in (2):

$$e_a = \widehat{a} \times a_p, \text{ where } \widehat{a} = \frac{{}^s a}{\| {}^s a \|}. \qquad (2)$$

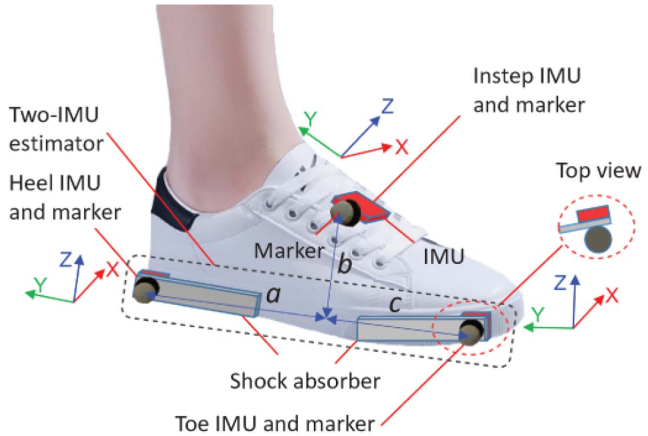

Figure 1. Overview of the developed multiple-IMU system and the placement of the IMUs and markers.

Table 1. Four estimators with different configurations of IMU.

Estimators	IMUs	Heel clearance	Toe clearance
Instep IMU	One	Indirect	Indirect
Toe IMU	One	Indirect	Direct
Heel IMU	One	Direct	Indirect
Two IMU	Two	Direct	Direct

Note: 'Direct' and 'Indirect' indicate that the foot clearance is estimated directly or indirectly.

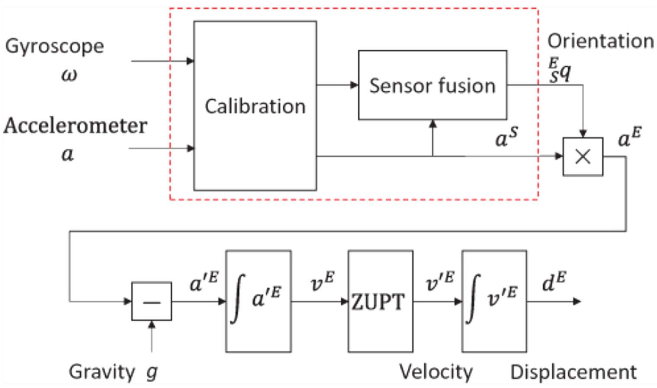

Figure 2. Overall schematic of the double integration method for sensor trajectory estimation.

Then the corrected angular velocity ω' is calculated as (3):

$$\omega' = {}^{S}\omega + K_a e_a. \tag{3}$$

K_a is the tuning parameter which regulates the weighting factor between the gyroscope and accelerometer measurement. A large value means it is trusting the accelerometer more, and typically it is determined experimentally through trial and error.

The rate of change of the quaternion, $\dot{q}$, is computed as

$$\dot{q} = \frac{1}{2} {}^{S}_{E}\hat{q} \otimes [\, 0 \; (\omega')^{T} \,]. \tag{4}$$

Then ${}^{S}_{E}q$ is calculated through the integration, as described in (5):

$${}^{S}_{E}q = \int \dot{q} \, \mathrm{d}t \tag{5}$$

$${}^{E}_{S}q = \left({}^{S}_{E}q\right)^{*}. \tag{6}$$

Here, ${}^{S}_{E}q$ describes the orientation of the earth frame relative to the sensor frame; the final orientation ${}^{E}_{S}q$ of the sensor frame relative to the earth frame can be obtained through the quaternion conjugate operation.

It is worth noting that the sensor calibration is also critical. The acceleration accuracy will affect the orientation estimation and the displacement estimation directly. The gyroscope accuracy will affect the displacement estimation indirectly. Although sensors are factory calibrated, calibration would still need to be checked at the end-user level. The scale factor and bias of the sensor can be updated using the method described in [26]. The gyroscope bias needs to be removed in sensor fusion methods. In this paper, for simplicity, we used the no-motion gyro bias update method to remove the bias, as depicted in our previous study [27].

2.2.2. The adaption of the filter gain. In the sensor fusion algorithm, it is crucial to regulate the filter gain K_a according to external acceleration. Human walking is a cyclic motion, and the gait events and gait phases during walking are shown in figure 3. The gait phases include the stance and swing phase; the gait events include toe off, heel strike, etc. The sensor fusion algorithm is concerned with the motion state of the sensor rather than the precise moment of gait events [25]. Hence, we simply divide the gait cycle into two states according to the motion state, i.e. the dynamic state and static state [16]. In the dynamic state, the foot is considered to be in a dynamic state with large external acceleration. In the static state, corresponding to the mid-stance phase, the foot is considered to be in a stationary state and the external acceleration is negligible.

The motion states are detected by the magnitude of the measured acceleration. To avoid sudden change, we first use a low-pass filter to filter the magnitude of acceleration and then compare the filtered magnitude with the gravity acceleration. When the deviation is smaller than a set threshold, it is regarded as a static state. Otherwise, it is a dynamic state. The

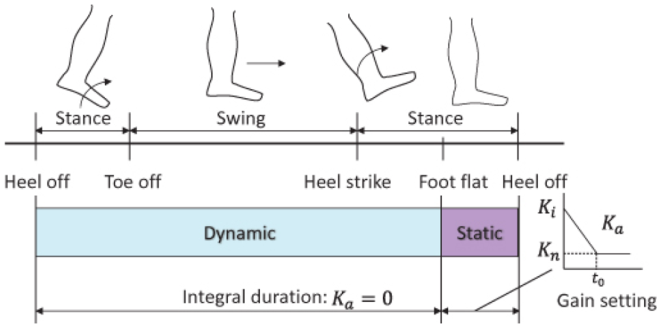

Figure 3. The gait phases and events during normal walking.

filter gain K_a is adaptively set according to the motion state. As shown in figure 3, in dynamic state, K_a is set to zero. Hence, the orientation estimation relies only on gyroscope integration. This period is called the integral duration. In static state, $e_a = \hat{a} \times a_p$, where $\hat{a} = \frac{{}^{s}a}{\|{}^{s}a\|}$ is set as a large initial value K_i for rapid convergence, and then is linearly decreased to normal value, K_n, in a time interval t_0. The static state is important to bound the drift of integration. Note that the static state occupies only about 20% of the gait cycle [28], and the convergence speed of the orientation estimation algorithms should be fast enough so that the orientation error due to the integration in the dynamic state can be corrected in such a short period.

2.3. Toe and heel trajectory estimation and feature extraction

2.3.1. 3D sensor trajectory estimation. In the process of double integration in sensor trajectory estimation, as shown in figure 2, the first step is to calculate the acceleration in the earth frame, ${}^{E}a(t)$, using the measured 3D acceleration ${}^{S}a(t)$ and the estimated orientation ${}^{E}_{S}q(t)$, and then to calculate the linear acceleration ${}^{E}a'(t)$ by subtracting the gravity acceleration g, as described in (7). Through integration, we get the 3D velocity ${}^{E}v(t)$. To avoid the accumulative error in acceleration integration, the zero-velocity update (ZUPT) method is used for the velocity correction [29]. During the static state, the IMU is in a static state, so the velocity of the sensor is set to zero, as described in (8). This known information is used to bound the error growth by correcting the velocity at the end of a dynamic state, v_{end}, to zero. The correction method is the linear de-drifting method, as described in (10) and (11) [30]. Finally, we get the 3D displacement ${}^{E}d(t)$ by integrating the corrected 3D velocity ${}^{E}v'(t)$, as described in (12):

$${}^{E}a'(t) = {}^{E}_{S}q(t) \cdot {}^{S}a(t) \cdot {}^{E}_{S}q'(t) - g. \tag{7}$$

In static state:

$${}^{E}v'(t) = {}^{E}v(t) = 0. \tag{8}$$

In dynamic state:

$${}^{E}v(t) = \int_{t_{start}}^{t_{end}} {}^{E}a'(t) \, \mathrm{d}t \tag{9}$$

$$v_{drift}(t) = \frac{(t - t_{start}) \cdot v_{end}}{t_{end} - t_{start}} \tag{10}$$

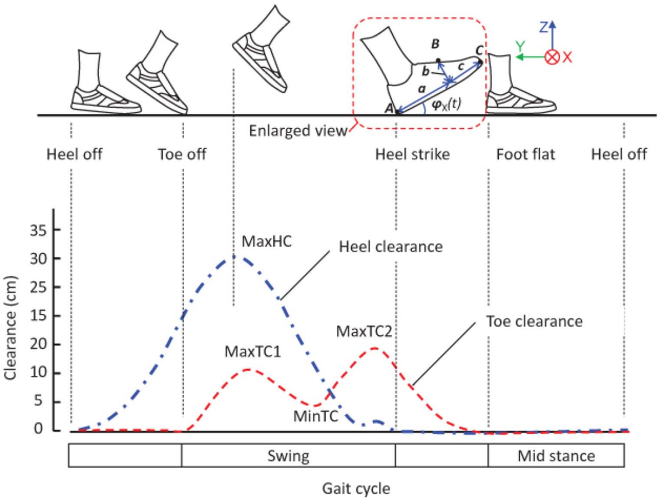

Figure 4. The heel and toe clearance in a normal gait and the definition of the four features (MaxHC, MaxTC1, MinTC and MaxTC2) of the foot clearance.

$$^{E}v'(t) = {}^{E}v(t) - v_{drift}(t) \tag{11}$$

where t_{start} and t_{end} are the start and the end of a dynamic state in a gait cycle, and v_{end} is the velocity at the end of a dynamic state before de-drifting:

$$^{E}d(t) = \int {}^{E}v'(t)\mathrm{d}t. \tag{12}$$

2.3.2. Toe and heel clearance calculation. For instep IMU, toe IMU and heel IMU estimators, we estimate the sensor trajectory first and then use geometric transformations to estimate the heel and toe clearances indirectly. In the two-IMU estimator, the toe IMU and heel IMU clearances are regarded as the toe and heel clearance. The indirect toe and heel clearance are calculated using geometric transformations presented in [13]. Specifically, for each estimator, the toe and heel clearance are calculated through (14)–(22), where A, B and C are the locations of the heel IMU, instep IMU and toe IMU, and *a, b* and *c* denote the relative distances between the IMUs, as shown in figure 4. $\varphi_X(t)$ is the shoe angle between the shoe sole and the ground. In the sagittal plane, it is linearly correlated to the roll angle of the IMUs for the X axis of the IMUs pointing left. The shoe angle can be calculated from the roll angle of the IMUs, as described in (13). To avoid discrepancy in IMU location estimation, we measured the locations (*a, b* and *c*) of the IMUs using the optical motion capture system instead of using the automatic estimation method presented in [13]. Hence, even the single IMU estimators in this paper avoided IMU location errors, and they should be more accurate than the original estimator presented in [13]:

$$\varphi_X(t) = -(\varphi(t) - \varphi_0) \tag{13}$$

where φ_0 is the roll angle of IMU in static state, which is regarded as the offset angle. $\varphi(t)$ is the roll angle during walking. $\varphi_X(t)$ is the shoe angle. The minus sign is to make the shoe angle positive at the moment of heel strike.

For the instep IMU estimator:

$$Z_{Instep}(t) = Z_{I\_IMU}(t) + b \tag{14}$$

$$Z_{Toe}(t) = Z_{Instep}(t) - b \cdot \cos\varphi_X(t) + c \cdot \sin\varphi_X(t) \tag{15}$$

$$Z_{Heel}(t) = Z_{Instep}(t) - b \cdot \cos\varphi_X(t) - a \cdot \sin\varphi_X(t). \tag{16}$$

For the heel IMU estimator:

$$Z_{Toe}(t) = Z_{H\_IMU}(t) + (a+c) \cdot \sin\varphi_X(t) \tag{17}$$

$$Z_{Heel}(t) = Z_{H\_IMU}(t). \tag{18}$$

For the toe IMU estimator:

$$Z_{Toe}(t) = Z_{T\_IMU}(t) \tag{19}$$

$$Z_{Heel}(t) = Z_{I\_IMU}(t) - (a+c) \cdot \sin\varphi_X(t). \tag{20}$$

For the two-IMU estimator:

$$Z_{Toe}(t) = Z_{T\_IMU}(t) \tag{21}$$

$$Z_{Heel}(t) = Z_{H\_IMU}(t) \tag{22}$$

where $Z_{Toe}(t)$ and $Z_{Heel}(t)$ are the calculated toe and heel clearance. $Z_{I\_IMU}(t)$, $Z_{T\_IMU}(t)$ and $Z_{H\_IMU}(t)$ are the vertical components of the trajectory of the instep, toe and heel IMU.

2.3.3. Feature extraction. In clinical gait analysis, the major interests are the features of the toe clearance and heel clearance. As shown in figure 4, there are four features in the foot clearance in a normal gait according to the definition in [13]. They are maximal heel clearance (MaxHC) right after toe-off, the first maximum toe clearance (MaxTC1), the minimal toe clearance (MinTC) in the dynamic state and the second maximum toe clearance (MaxTC2) before heel strike. In these features, the most important feature is the MinTC, for it relates to tripping and safety in obstacle negotiation [8]. There are also a few studies focusing on the significance of the other three features. For example, Dadashi *et al* reported that the age effect was also significant for MaxHC and MaxTC1, and the study of MaxTC1 and MaxTC2 revealed strategies in the toe-off control and obstacle negotiation [31]. For completeness, we analyzed all four features of foot clearance. The features (MaxHC, MaxTC1, MinTC and MaxTC2) are extracted by finding the maximum or minimum from the estimated heel and toe clearance. All the features are calculated in each step, and the height at the end of the previous step is regarded as the offset height when calculating the foot clearance features.

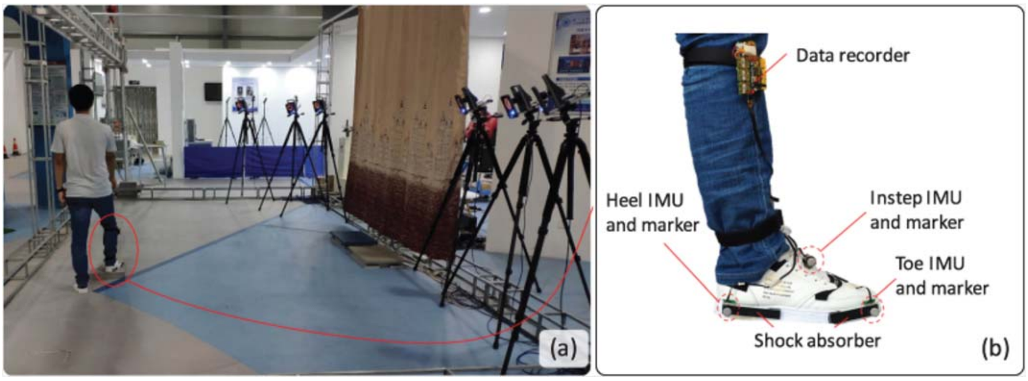

Figure 5. (a) The scenario of the validation experiment. (b) The prototype of the IMU system and the placements of the IMUs and markers.

3. Experimental validation

In this section, we validated the proposed foot clearance estimation method through walking experiments. The IMU system was developed with commercially available IMU modules. As shown in figure 5, it contained three IMU modules (MTi-3-8A7G6, XSENS B.V. Technologies, Enschede, Netherlands), a data recorder and a remote controller. The IMU modules were encased in a PLCC28 socket, and the size was 18×18×5 mm, which could be easily fixed onto the shoe. The data recorder was used to record the output data of the three IMU modules in three SD cards synchronously. The data recorder contained a 1200 mAh li-ion battery, providing about five hours of battery life. The remote controller controlled the start and the stop of recording. A six-camera optical motion capture system (Vicon T40 s, Oxford, UK) served as the gold standard of the foot clearance. There was also another receiver connected to the trig-in port of the Vicon host to synchronize the data collection of the IMU system and Vicon system. All the data from Vicon and the IMU systems were processed offline in MATLAB (MathWorks Inc., Natick, MA, USA).

We recruited eight healthy male subjects for this study (age 25.3 ± 4.2 years, height 179 ± 4.5 cm, mass 70.1 ± 4.2 kg, EUR. shoe size 42.1 ± 1.1). Informed consent was obtained from each subject prior to the experiment, and the study was approved by the ethical committee at Zhejiang University. During the experiments, the recorder was attached to the shank of the subject using a Velcro strap. The experimental scenario is shown in figure 5(a) and the placements of IMUs and markers are shown in figure 5(b). The details of the IMU system are described in section 2. All six cameras for the motion capture were placed on one side to maximize the capture area. To acquire the reference height of the IMU, we placed the markers close to the center of the IMUs at the same height. Thus, instrument error could be minimized. The scale factor and bias of the accelerometers were re-calibrated using the method described in [26]. In addition, in the proposed foot clearance estimation methods, the threshold for static detection was set as 0.025 g. K_a was set to 5, and was then linearly decreased to 0.5 within 0.2 s, to ensure rapid convergence of the orientation during static state.

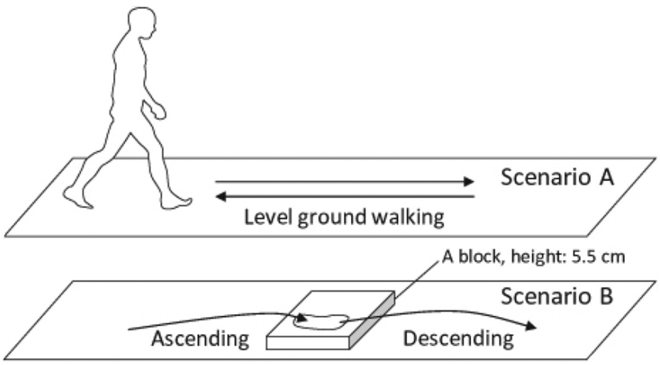

Figure 6. The test scenario of level ground walking with different speeds (scenario A) and uneven ground walking (scenario B).

3.1. Experimental protocol

To investigate the effects of different walking conditions, the proposed method was evaluated under four normal walking and three imitative pathological walking conditions. The normal walking conditions included uneven ground walking and level ground walking at three different speeds. Figure 6 shows the scenario of the tests. The speeds of level ground walking were slow (0.8–1.0 m s^{-1}), normal (1.0–1.2 m s^{-1}), and fast (1.2–1.4 m s^{-1}). In the uneven ground walking test, the subjects were instructed to walk up and down a block with a preferable speed, and the height of the block was 5.5 cm. In the pathological walking experiments, the subjects were trained to mimic ataxic gait, waddling gait and Parkinsonian gait. We trained the subjects using a standard pathological gait video and demonstration. The step sequence of each gait is shown in figure 7. In normal gait, the step width is moderate and the stride length is long. In ataxic gait, the subjects will not be able to walk in a straight line because of cerebellar disease, so they walk in a zigzag shape. In waddling gait, because of hip girdle muscle weakness on one side, the subjects will drop in the pelvis on the contralateral side of the pelvis while walking, leading to waddling. In Parkinsonian gait, the subjects take jerky steps, and the strides become quicker and shorter than in normal gait [3]. In each trial of the experiment, the subject was asked to stand still for about 20 s, so the gyroscope bias could be removed by subtracting the mean of the gyroscope

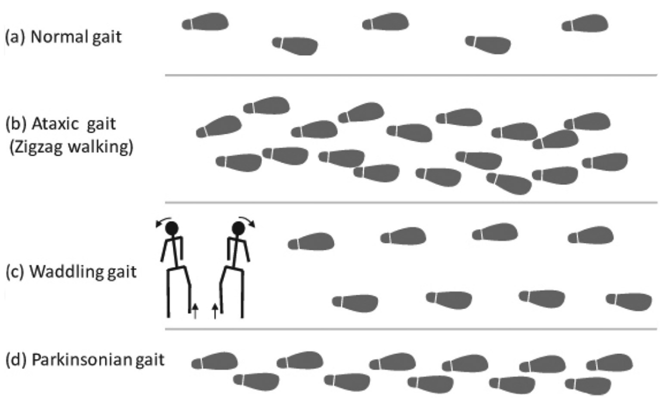

Figure 7. Graphic representation of the step sequence in normal gait and three pathological gaits. (a) Normal gait, regular steps. (b) Ataxic gait, zigzag walking. (c) Waddling gait, broadened base. (d) Parkinsonian gait, quicker and shorter steps.

output. Then, the subject walked straight in the motion capture volume about four steps. Each walking trial was repeated about 25 times. Considering the limited capture volume, we discarded the initiation and termination part of the gaits in each trial. The intermediate two steps were regarded as valid steps, and thus we got about 40–50 valid gait cycles under each walking condition.

3.2. Data analysis

We extracted the features (MaxHC, MaxTC1, MinTC, MaxTC2) from the heel and toe clearance estimated by IMU and Vicon. The features from Vicon were regarded as the reference. For easy comparison with different accuracy representations in the literature, the mean, standard deviation and the root mean square error (RMSE) of MaxHC, MaxTC1, MinTC and MaxTC2 were all calculated. The limit of agreement (LOA) of the proposed IMU system with different estimators and the Vicon system was also assessed using the Bland and Altman graphical method.

4. Results

4.1. Foot clearance estimation using different estimators

The heel and toe clearance of one typical participant (Subject 5) are shown in figure 8. There were two consecutive gait cycles of normal gait with level ground walking, normal gait with uneven ground walking, waddling gait, ataxic gait and Parkinsonian gait. The foot clearances were estimated by the two-IMU estimator and Vicon. For easy calculation of the relative foot clearance in each gait cycle, we manually aligned the foot clearance of IMU estimators and Vicon in the middle of the static state. As can be seen from the figure, the foot clearance in normal gait was regular and the MaxHC was higher than with pathological gaits; the MaxHC with Parkinsonian gait was much smaller than with the other gaits, which was in accordance with the symptoms of quicker and shorter steps.

We extracted a total of 2640 gait cycles (8 subjects $\times$ 7 conditions $\times$ 40–50 gait cycles). The gait cycles were different because of the gait cycle variability in subjects during the experiments. To compare the accuracy of the different estimators, we analyzed the foot clearance from different estimators. The mean, standard deviation and RMSEs of the four features of each estimator are listed in table 2. In the two-IMU estimator, the mean, standard deviation and RMSE of MaxHC and MinTC were -0.34 ± 0.24 cm, 0.42 cm and 0.02 ± 0.26 cm, 0.26 cm, and those of MaxTC1 and MaxTC2 were -0.13 ± 0.24 cm, 0.27 cm and -0.03 ± 0.35 cm, 0.35 cm. All the RMSEs were below 1 cm, achieving better accuracy than the heel IMU and instep IMU estimators. The Bland and Altman plots of all the features of foot clearance estimated by different estimators are shown in figure 9, and the mean of the differences and ± 1.96 standard deviation were plotted to illustrate the bias and the LOA (95% confidence intervals) between the IMUs and Vicon system. It can be seen that the MinTC contained many negative values and large values (>10 cm). The negative values appeared when the subject walked down from the block, and the large values appeared when the subject walked up to the block. By comparing four estimators, we can see that the LOA of the two-IMU estimator (black line) was the smallest. The toe IMU estimator (green line) also performed well in terms of the accuracy of MaxHC; the RMSE was just 0.70 cm. However, the good results relied on the accurate measurement of IMU locations and the placement, and the standard deviation was larger than that of the two-IMU estimator. Therefore, the two-IMU estimator was found to be the best estimator.

4.2. Influence of walking speed on foot estimation

As the two-IMU estimator represents the best estimator, we only present the results of the two-IMU estimator in the following subsections for simplicity. The accuracy of the foot clearance in slow (0.8–1.0 m s^{-1}), normal (1.0–1.2 m s^{-1}), fast walking (1.2–1.4 m s^{-1}), uneven ground walking conditions and pathological gaits are listed in table 3. The results of each condition were calculated from the gait cycles of all the subjects. It can be seen that for the first six walking conditions, the differences were small in the error of MaxHC, MaxTC1, MinTC and MaxTC2, while for Parkinsonian gait, the error was smaller than with the other conditions. This can be explained by the fact that total foot clearance was much smaller with this than with other gaits, as shown in figure 8(e), and thus achieved smaller error at a certain percentage error.

4.3. The intra-subject variability in foot clearance accuracy

As the walking pattern of different subjects may be different, it is necessary to analyze the foot clearance accuracy between different subjects. In the appendix, we list the accuracy of all the subjects walking in different conditions. For normal gait, as in tables A1–A4, it can be seen that the accuracy varies between subjects. For example, in table A1, for subject 2 in

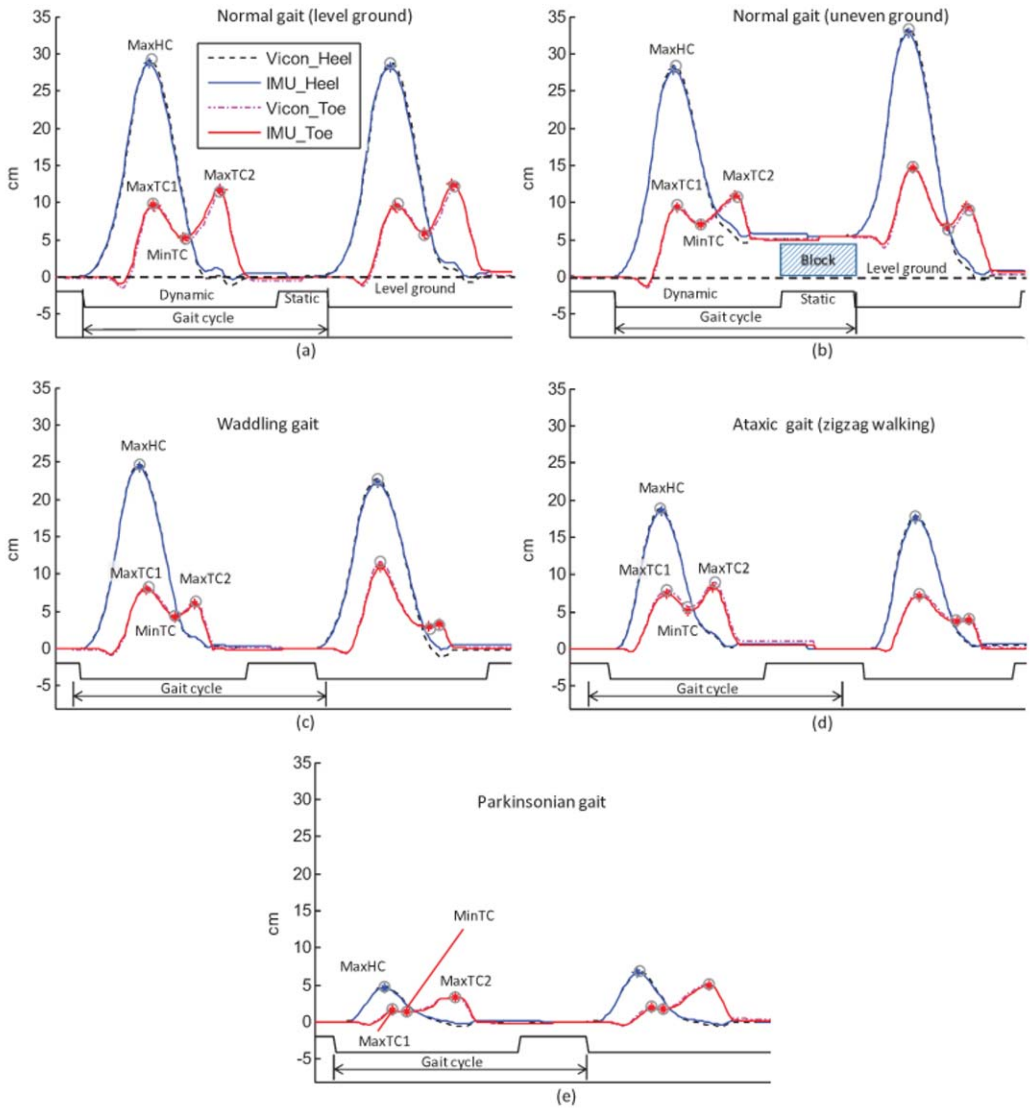

Figure 8. An example of the heel and toe clearance estimated by two-IMU estimator and Vicon. (a) Level ground walking, (b) uneven ground walking, (c) waddling gait, (d) ataxic gait, (e) Parkinsonian gait.

Table 2. The accuracy of foot clearance estimated by different estimators.

	MaxHC (cm)		MaxTC1 (cm)		MinTC (cm)		MaxTC2 (cm)	
Estimators	Mean ± SD	RMSE	Mean ± SD	RMSE	Mean ± SD	RMSE	Mean ± SD	RMSE
Instep IMU	-0.21 ± 1.16	1.18	-1.35 ± 0.95	1.65	-0.28 ± 0.63	0.69	0.83 ± 0.75	1.12
Toe IMU	0.51 ± 0.48	0.70	-0.13 ± 0.24	0.27	0.02 ± 0.26	0.26	-0.03 ± 0.35	0.35
Heel IMU	-0.34 ± 0.24	0.42	-1.19 ± 0.54	1.31	-0.95 ± 0.60	1.13	-0.06 ± 0.76	0.77
Two IMU	$\mathbf{-0.34 \pm 0.24}$	**0.42**	$\mathbf{-0.13 \pm 0.24}$	**0.27**	$\mathbf{0.02 \pm 0.26}$	**0.26**	$\mathbf{-0.03 \pm 0.35}$	**0.35**

the fast walking condition, the RMSE of MaxHC was 0.93 cm, which was much higher than others. In table A2, for subject 6 in the normal walking condition, the RMSEs of MinTC and MaxTC2 were 0.42 cm and 0.53 cm, which were larger than those of other subjects. However, for imitative pathological gaits, as shown in tables A5–A7, the results show good consistency between subjects.

5. Discussion

5.1. The accuracy of the estimated foot clearance

In this study, we aimed at understanding the limiting factors in foot clearance estimation when using low-cost IMUs. Through the improvements in sensor fusion algorithm, sensor

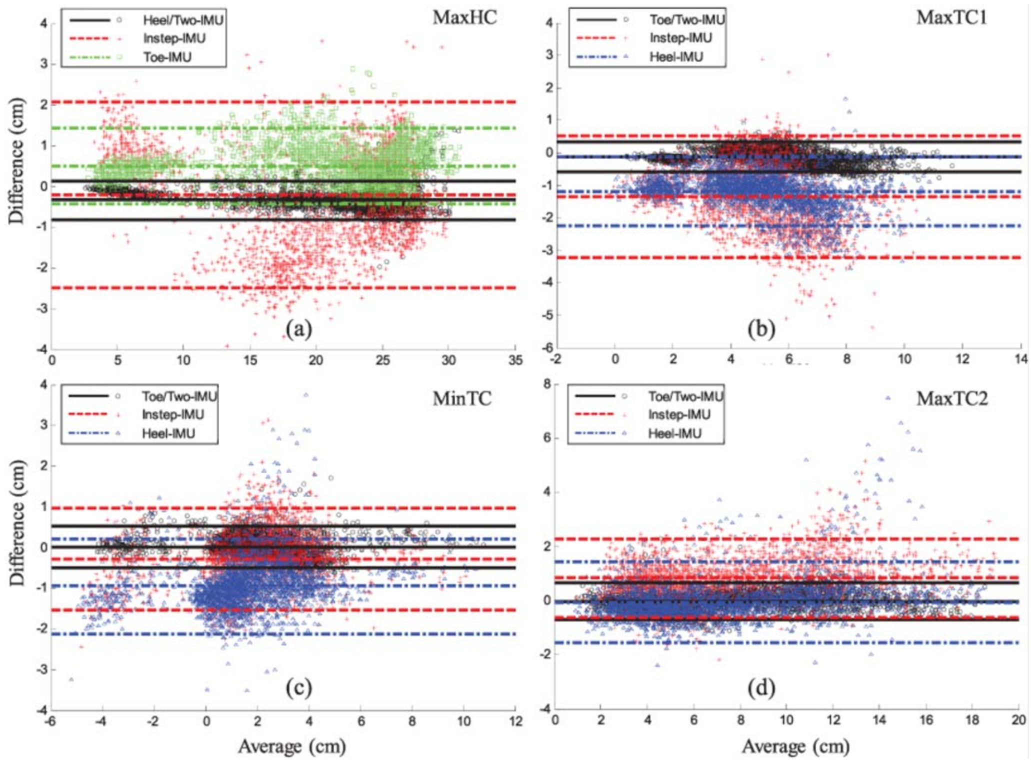

Figure 9. Bland and Altman plots of the mean ±1.96 SD LOA of foot clearance features of all the 2640 gait cycles estimated by four different estimators. (a) MaxHC, (b) MaxTC1, (c) MinTC, (d) MaxTC2. Different estimators are marked with different markers and line type. The black line indicates the LOA of two-IMU estimator, which achieved the best accuracy.

Table 3. The accuracy of the foot clearance in different walking conditions using two-IMU estimator.

	MaxHC (cm)		MaxTC1 (cm)		MinTC (cm)		MaxTC2 (cm)	
Type	Mean ± SD	RMSE	Mean ± SD	RMSE	Mean ± SD	RMSE	Mean ± SD	RMSE
Fast	−0.38 ± 0.36	0.53	−0.00 ± 0.19	0.19	0.13 ± 0.24	0.27	0.09 ± 0.34	0.35
Normal	−0.43 ± 0.21	0.48	0.02 ± 0.19	0.19	0.14 ± 0.22	0.26	0.13 ± 0.28	0.31
Slow	−0.43 ± 0.18	0.46	0.04 ± 0.14	0.15	0.13 ± 0.18	0.22	0.11 ± 0.24	0.26
Uneven	−0.44 ± 0.21	0.48	−0.01 ± 0.15	0.15	0.14 ± 0.34	0.36	0.04 ± 0.35	0.35
Ataxic	−0.25 ± 0.28	0.37	−0.33 ± 0.24	0.41	−0.11 ± 0.28	0.30	−0.21 ± 0.38	0.43
Waddling	−0.32 ± 0.11	0.34	−0.39 ± 0.16	0.42	−0.16 ± 0.29	0.33	−0.23 ± 0.39	0.45
Parkinson	−0.17 ± 0.10	0.19	−0.20 ± 0.08	0.21	−0.09 ± 0.10	0.13	−0.13 ± 0.17	0.22

placement and shock absorption, we improved the accuracy in foot clearance estimation. From the results in table 2, we can see that for the two-IMU estimator, the achieved accuracy of MaxHC and MinTC was -0.34 ± 0.24 cm and 0.02 ± 0.26 cm, and the corresponding RMSEs were 0.42 cm and 0.26 cm. All of them were below 1 cm, showing high accuracy and precision. The accuracy comparison between different studies and the features of each study are summarized in table 4. The accuracy of the estimated foot clearance in [13] was only centimeter level. The RMSE in [22] was much smaller, but the results relied on the machine learning approach, and the models for different groups of subjects were different. Kitagawa and Ogihara also achieved good accuracy, but the method relied on the flat floor assumption, and the estimated clearance was the clearance of instep IMU rather than the biomechanical heel and toe clearance [14]. In the method presented in [18], the range sensor was added, data-driven models were used to correct the foot clearance, and the flat floor assumption was also required. In this paper, the proposed improved method with two-IMU configuration (two-IMU estimator) showed better accuracy. It did not rely on any post-estimation correction or any data-driven models, i.e. it did not rely on a subject-specific training dataset and can be easily used in real-time systems. Moreover, it also did not rely on the flat floor assumption, and thus could be used for uneven ground walking; the results in table 3 show that it achieved equivalent accuracy to level ground walking. Systematic biases are observed

Table 4. The accuracy comparison between different studies.

Study	MaxHC (cm)		MinTC (cm)	
	Mean ± SD	RMSE	Mean ± SD	RMSE
Mariani *et al* [13]	4.1 ± 2.3	-	1.3 ± 0.9	-
Santhiranayagam *et al* [22]	-	-	-	0.66
Kitagawa and Ogihara [14]	-	-	0.2 ± 0.7	-
Arami *et al* [18]	0.08 ± 0.75	-	0.09 ± 0.61	-
Two-IMU estimator	$\mathbf{-0.34 \pm 0.24}$	**0.42**	$\mathbf{0.02 \pm 0.26}$	**0.26**

Note: '-' denotes information not available in the literature.

in MaxHC; as shown in figure 9(a), most of the estimated MaxHCs were smaller than the reference. The accuracy can be further improved if post-estimation correction is performed.

Interestingly, in table 2, the error of MaxHC of the toe IMU estimator was just 0.51 ± 0.48 cm, which was comparable with the -0.34 ± 0.24 cm from the two-IMU estimator. However, the results were based on accurate IMU locations measured by Vicon. Inaccurate estimation of the locations would enlarge the error of the MaxHC. The results in table 3 show that different walking speeds and uneven ground conditions do not show large differences. A plausible interpretation is that as long as the static state is successfully detected, the accuracy of the foot clearance is reliable. The results in tables A1–A4 in the appendix show that gait variability has an impact on the accuracy of foot clearance. A reasonable interpretation is that the stability of the toe or heel of different subjects is different. As the ZUPT is based on the assumption of zero velocity, if the velocity of the IMU is forced to be corrected to zero with an initial velocity, velocity error will be introduced, thus enlarging the foot clearance estimation error. However, the results in tables A5–A7 show good consistency between subjects.A plausible explanation is that because all the subjects were trained from the same demonstration video, the similar imitative gait pattern may cause it. Considering the diversity of the pathological gaits, the presented method should be validated with patients in the future.

In the presented IMU-based 3D foot trajectory estimation method, the orientation and the displacement estimations are both continuous, while in the studies [13, 14, 18], orientation and displacement reset were required and the displacement was estimated in each step. Compared with these studies, the method in this paper could potentially be used for continuous gait tracking under various conditions, including stairs, slopes and uneven ground walking.

5.2. Orientation estimation and its effects on foot clearance calculation

According to the above analysis, the orientation accuracy is important for foot clearance estimation because it determines the accuracy of motion acceleration that is used for double integration. Based on our previous study, the angular velocity integration error in a dynamic state (1–2 s) is negligible [27]. Hence, the orientation error is mainly caused by the initial error before the integration period, i.e. the orientation error in static state. Therefore, the key to the sensor fusion is to ensure the orientation converges to the orientation calculated from the acceleration in static state timely, because the orientation calculated from the acceleration is more reliable in static state. Otherwise, the accumulative orientation error cannot be eliminated and will become significant especially in the continuous walking condition, and thus decrease the accuracy in the following foot clearance estimation. In particular, we estimate the orientation through the sensor fusion algorithm instead of using the orientation calculated from the acceleration directly, because it ensures the continuity and the smoothness of the orientation estimation. Thus, the estimated orientation can also be used in continuous foot trajectory estimation.

5.3. Necessary factors for accurate foot clearance estimation

Through this study, we understood the necessary factors for achieving high precision as follows:

(a) Sensor calibration: The displacement estimation is the basis of the foot clearance estimation, which is calculated by double integration of acceleration. Accurate displacement estimation is more demanding in accelerometer calibration than orientation estimation. Although the IMUs are factory calibrated, they should be carefully checked before being used for foot clearance estimation.
(b) The orientation estimation algorithm: Similarly, the sensor orientation determines the accuracy of motion acceleration after subtracting the gravity acceleration. Foot clearance estimation also demands a high orientation estimation accuracy. In the optimized sensor fusion process, the convergence speed in static state is critical. If the convergence is not fast enough, the accumulative error cannot be removed in the short interval, thus degrading the accuracy of the estimated orientation.
(c) Shock absorber: Shock absorption is a commonly used method in accelerometer-based displacement estimation. This can be explained by the fact that the measurement error of an accelerometer is usually within a certain percentage. The absolute error increases with the magnitude of acceleration, which means larger acceleration contains a bigger absolute error. Therefore, attenuating large acceleration can improve the accuracy of acceleration and also

avoid exceeding the full-scale range of an accelerometer, thus improving the displacement estimation indirectly. To attenuate the shock of the IMUs, we fixed the IMUs to the middle of the shoe sole through a plastic shock absorber. Hence, the shock of the IMU was equivalent to the middle of the shoe sole, which avoided the strong shock at the toe and heel of the shoe sole but still estimated the toe and heel clearance. According to our primary tests, the absorber attenuated the peak acceleration occurring at the moment of heel strike or toe-off and had no effect on acceleration during the swing phase, and the RMSEs of estimated foot clearance were improved.

(d) The installation direction of the sensor: For MEMS-based IMUs, the accelerometers in each axis are different due to the sensor variability. When used in foot clearance estimation, it is necessary to find the most suitable installation direction through trial and error tests.

5.4. The method of using two independent IMUs

In single-IMU-based foot clearance estimations, as in [13, 19], the IMU location estimation relied on accurate gait event detection and the assumption that the heel clearance was zero at the event of heel strike. The geometric transformations require accurate shoe angle estimation and no relative motion between the IMU and shoe. Any errors in these intermediate calculations would enlarge the error in foot clearance estimation. However, in the two-IMU estimator, two independent IMUs were used for toe and heel clearance estimation. This avoided intermediate calculations errors, and thus achieved better accuracy than the single-IMU indirect methods. Therefore, a direct foot clearance estimator is recommended.

In short, the proposed method with the two-IMU estimator has several advantages. First, the proposed method does not rely on accurate gait phase detection, and thus it has the potential to be used in abnormal gaits. Second, it does not depend on the hypothesis of a horizontal surface, thus it can be used on stairs and for uneven ground walking. Third, foot clearance is directly estimated by the double integration method. The results do not rely on any data-driven models [18] or machine learning method depending on specific training [22], thus, it is more applicable. Moreover, the proposed method can potentially serve as a general foot trajectory estimation method; more gait parameters can also be extracted from the estimated position, such as stride length, step width, etc.

The proposed method also has some limitations. The installation direction of each sensor needs to be fine-tuned; a change of sensor may need an additional initial tuning procedure. The shock absorber still needs further improvement for it may easily collide with other things in our daily life environments. Although the pathological walking conditions were included in the experiments, they were imitative pathological gaits of healthy subjects, which might not fully represent real pathological gaits. In the future, the method should be validated with patients.

6. Conclusions

This paper developed a set of procedures to improve the key components in foot clearance estimation, by considering orientation estimation, sensor placement and shock absorption. The improved method was validated through walking experiments under different conditions, including normal gait and imitative pathological gaits. The mean and standard deviation of MaxHC and MinTC were -0.34 ± 0.24 cm and 0.02 ± 0.26 cm, which was more accurate than previous studies but required fewer preconditions. The results demonstrate that it is possible to achieve reliable millimeter-level accuracy in foot clearance estimation using only IMUs. The method may also be suitable for uneven ground walking as well as three kinds of imitative pathological gaits, without the dependence on any data-driven models or any post-estimation correction. Accurate foot clearance estimation using an inertial sensor is significant for fall risk assessment in the daily living environment. In addition, the presented improved method has the potential for accurate gait tracking and extraction of other spatial gait parameters. In the future, the proposed method will be extended to real-time biofeedback and gait retraining applications.

Acknowledgments

This work was supported in part by the NSFC under Grant Nos. 51775485 and U1613203, and the Zhejiang Provincial Natural Science Foundation of China under Grant No. LZ20E050002. We also acknowledge all the participants who contributed to this study. The authors have confirmed that any identifiable participants in this study have given their consent for publication.

Author contribution

Bingfei Fan contributed to the original concept; study conception and design; data processing, analysis and interpretation; and manuscript drafting and revision. Qingguo Li contributed to the original concept; supervision of the work; manuscript drafting and revision; and manuscript critical revision. Tao Liu contributed to the original concept; supervision of the work; and manuscript critical revision.

Conflicts of interest

The authors declare no conflict of interest.

Appendix

In this appendix, the accuracy of the foot clearance of different subjects is listed in the following tables. The foot clearance was estimated by two-IMU estimator and the conditions included fast, normal and slow speed level ground walking conditions and uneven ground walking condition.

Table A1. The accuracy of the foot clearance features between different subjects using two-IMU estimators in fast walking condition.

	MaxHC (cm)		MaxTC1 (cm)		MinTC (cm)		MaxTC2 (cm)	
Subject	Mean ± SD	RMSE	Mean ± SD	RMSE	Mean ± SD	RMSE	Mean ± SD	RMSE
1	−0.33 ± 0.11	0.35	0.08 ± 0.14	0.16	0.11 ± 0.14	0.17	0.04 ± 0.19	0.20
2	**−0.86 ± 0.35**	**0.93**	0.06 ± 0.10	0.11	−0.01 ± 0.14	0.14	−0.11 ± 0.19	0.21
3	−0.41 ± 0.15	0.44	0.00 ± 0.13	0.13	0.08 ± 0.24	0.24	−0.09 ± 0.29	0.31
4	−0.38 ± 0.22	0.44	0.33 ± 0.13	0.35	0.31 ± 0.17	0.36	0.23 ± 0.23	0.32
5	−0.30 ± 0.20	0.36	−0.22 ± 0.10	0.24	0.30 ± 0.15	0.33	0.41 ± 0.21	0.46
6	−0.03 ± 0.68	0.67	−0.12 ± 0.10	0.15	0.32 ± 0.23	0.39	0.43 ± 0.29	0.52
7	−0.51 ± 0.15	0.53	−0.07 ± 0.10	0.12	0.03 ± 0.19	0.19	−0.04 ± 0.30	0.30
8	−0.32 ± 0.09	0.33	−0.08 ± 0.13	0.15	−0.09 ± 0.20	0.21	−0.19 ± 0.30	0.36

Table A2. The accuracy of the foot clearance features between different subjects using two-IMU estimators in normal walking condition.

	MaxHC (cm)		MaxTC1 (cm)		MinTC (cm)		MaxTC2 (cm)	
Subject	Mean ± SD	RMSE	Mean ± SD	RMSE	Mean ± SD	RMSE	Mean ± SD	RMSE
1	−0.41 ± 0.16	0.44	0.06 ± 0.12	0.13	0.02 ± 0.16	0.17	0.00 ± 0.21	0.20
2	−0.64 ± 0.13	0.66	0.10 ± 0.14	0.17	0.01 ± 0.20	0.20	−0.02 ± 0.28	0.28
3	−0.44 ± 0.10	0.45	0.02 ± 0.21	0.21	0.09 ± 0.29	0.30	0.01 ± 0.35	0.35
4	−0.45 ± 0.23	0.50	0.31 ± 0.12	0.33	0.35 ± 0.15	0.38	0.33 ± 0.19	0.37
5	−0.40 ± 0.12	0.41	−0.22 ± 0.07	0.23	0.21 ± 0.10	0.23	0.27 ± 0.14	0.31
6	−0.34 ± 0.42	0.53	−0.01 ± 0.10	0.10	**0.38 ± 0.17**	**0.42**	**0.51 ± 0.16**	**0.53**
7	−0.48 ± 0.12	0.49	−0.01 ± 0.08	0.08	0.15 ± 0.09	0.17	0.15 ± 0.13	0.20
8	−0.31 ± 0.10	0.32	−0.06 ± 0.11	0.12	−0.01 ± 0.12	0.12	−0.05 ± 0.16	0.17

Table A3. The accuracy of the foot clearance features between different subjects using two-IMU estimators in slow walking condition.

	MaxHC (cm)		MaxTC1 (cm)		MinTC (cm)		MaxTC2 (cm)	
Subject	Mean ± SD	RMSE	Mean ± SD	RMSE	Mean ± SD	RMSE	Mean ± SD	RMSE
1	−0.39 ± 0.17	0.43	0.12 ± 0.10	0.15	0.07 ± 0.14	0.15	0.05 ± 0.14	0.15
2	−0.63 ± 0.08	0.64	0.15 ± 0.07	0.16	0.08 ± 0.12	0.14	0.14 ± 0.17	0.22
3	−0.51 ± 0.09	0.52	0.07 ± 0.13	0.15	0.09 ± 0.22	0.23	−0.00 ± 0.31	0.30
4	−0.46 ± 0.14	0.48	0.15 ± 0.09	0.17	0.21 ± 0.18	0.28	0.08 ± 0.16	0.18
5	−0.32 ± 0.10	0.33	−0.19 ± 0.06	0.19	0.17 ± 0.10	0.19	0.16 ± 0.11	0.19
6	−0.42 ± 0.31	0.52	0.08 ± 0.11	0.14	0.31 ± 0.18	0.35	0.47 ± 0.21	0.51
7	−0.38 ± 0.12	0.40	0.06 ± 0.08	0.10	0.21 ± 0.08	0.22	0.22 ± 0.12	0.25
8	−0.32 ± 0.08	0.33	−0.05 ± 0.07	0.09	−0.04 ± 0.08	0.09	−0.14 ± 0.11	0.18

Table A4. The accuracy of the foot clearance features between different subjects using two-IMU estimators in uneven ground walking condition.

	MaxHC (cm)		MaxTC1 (cm)		MinTC (cm)		MaxTC2 (cm)	
Subject	Mean ± SD	RMSE	Mean ± SD	RMSE	Mean ± SD	RMSE	Mean ± SD	RMSE
1	−0.28 ± 0.18	0.33	0.06 ± 0.10	0.11	0.04 ± 0.12	0.12	0.03 ± 0.17	0.17
2	−0.66 ± 0.18	0.68	0.03 ± 0.10	0.11	−0.04 ± 0.13	0.13	−0.09 ± 0.25	0.26
3	−0.50 ± 0.11	0.51	−0.00 ± 0.18	0.18	0.09 ± 0.27	0.28	−0.05 ± 0.35	0.35
4	−0.45 ± 0.21	0.49	0.10 ± 0.21	0.23	0.36 ± 0.27	0.45	−0.13 ± 0.27	0.30
5	−0.46 ± 0.11	0.47	−0.04 ± 0.09	0.10	0.51 ± 0.56	0.76	0.51 ± 0.20	0.54
6	−0.37 ± 0.32	0.48	−0.05 ± 0.13	0.14	0.22 ± 0.25	0.33	0.36 ± 0.33	0.49
7	−0.43 ± 0.13	0.45	−0.07 ± 0.08	0.11	0.07 ± 0.08	0.11	0.11 ± 0.13	0.17
8	−0.32 ± 0.12	0.34	−0.13 ± 0.10	0.16	−0.12 ± 0.13	0.17	−0.30 ± 0.20	0.36

Table A5. The accuracy of the foot clearance features between different subjects using two-IMU estimators in ataxic gait.

	MaxHC (cm)		MaxTC1 (cm)		MinTC (cm)		MaxTC2 (cm)	
Subject	Mean ± SD	RMSE	Mean ± SD	RMSE	Mean ± SD	RMSE	Mean ± SD	RMSE
1	-0.33 ± 0.14	0.35	-0.35 ± 0.17	0.39	0.05 ± 0.33	0.33	0.06 ± 0.41	0.41
2	-0.08 ± 0.25	0.26	-0.22 ± 0.24	0.33	-0.01 ± 0.24	0.24	-0.06 ± 0.34	0.34
3	-0.11 ± 0.34	0.36	-0.22 ± 0.28	0.36	-0.11 ± 0.22	0.25	-0.27 ± 0.34	0.43
4	-0.35 ± 0.15	0.38	-0.39 ± 0.21	0.44	-0.05 ± 0.38	0.38	-0.20 ± 0.49	0.53
5	-0.32 ± 0.29	0.44	-0.38 ± 0.24	0.44	-0.25 ± 0.21	0.33	-0.43 ± 0.38	0.57
6	-0.31 ± 0.30	0.43	-0.39 ± 0.20	0.43	-0.18 ± 0.22	0.28	-0.22 ± 0.28	0.35
7	-0.25 ± 0.28	0.37	-0.34 ± 0.29	0.45	-0.13 ± 0.26	0.28	-0.23 ± 0.34	0.41
8	-0.27 ± 0.24	0.36	-0.30 ± 0.25	0.39	-0.20 ± 0.19	0.27	-0.32 ± 0.16	0.36

Table A6. The accuracy of the foot clearance features between different subjects using two-IMU estimators in waddling gait.

	MaxHC (cm)		MaxTC1 (cm)		MinTC (cm)		MaxTC2 (cm)	
Subject	Mean ± SD	RMSE	Mean ± SD	RMSE	Mean ± SD	RMSE	Mean ± SD	RMSE
1	-0.28 ± 0.11	0.30	-0.22 ± 0.09	0.24	0.05 ± 0.18	0.19	0.10 ± 0.22	0.23
2	-0.29 ± 0.11	0.31	-0.30 ± 0.11	0.31	0.02 ± 0.17	0.17	0.04 ± 0.20	0.20
3	-0.29 ± 0.12	0.31	-0.26 ± 0.18	0.32	-0.03 ± 0.45	0.44	-0.01 ± 0.58	0.57
4	-0.34 ± 0.10	0.36	-0.52 ± 0.10	0.53	-0.22 ± 0.17	0.28	-0.42 ± 0.20	0.46
5	-0.40 ± 0.09	0.41	-0.44 ± 0.09	0.45	-0.33 ± 0.15	0.37	-0.53 ± 0.20	0.57
6	-0.30 ± 0.10	0.31	-0.42 ± 0.13	0.44	-0.20 ± 0.23	0.30	-0.24 ± 0.30	0.38
7	-0.38 ± 0.11	0.40	-0.50 ± 0.14	0.52	-0.25 ± 0.30	0.39	-0.36 ± 0.38	0.52
8	-0.28 ± 0.06	0.28	-0.40 ± 0.10	0.41	-0.27 ± 0.27	0.39	-0.33 ± 0.32	0.45

Table A7. The accuracy of the foot clearance features between different subjects using two-IMU estimators in Parkinsonian gait.

	MaxHC (cm)		MaxTC1 (cm)		MinTC (cm)		MaxTC2 (cm)	
Subject	Mean ± SD	RMSE	Mean ± SD	RMSE	Mean ± SD	RMSE	Mean ± SD	RMSE
1	-0.31 ± 0.08	0.32	-0.24 ± 0.07	0.25	-0.00 ± 0.13	0.13	0.00 ± 0.18	0.17
2	-0.11 ± 0.07	0.13	-0.16 ± 0.04	0.17	-0.10 ± 0.07	0.12	-0.08 ± 0.09	0.12
3	-0.24 ± 0.07	0.25	-0.11 ± 0.04	0.12	-0.04 ± 0.06	0.07	-0.01 ± 0.09	0.09
4	-0.15 ± 0.06	0.16	-0.24 ± 0.07	0.25	-0.09 ± 0.07	0.11	-0.18 ± 0.10	0.20
5	-0.18 ± 0.08	0.20	-0.26 ± 0.10	0.27	-0.18 ± 0.10	0.20	-0.36 ± 0.15	0.39
6	-0.11 ± 0.05	0.12	-0.21 ± 0.06	0.21	-0.09 ± 0.07	0.12	-0.16 ± 0.11	0.20
7	-0.17 ± 0.07	0.18	-0.17 ± 0.09	0.20	-0.07 ± 0.12	0.14	-0.09 ± 0.18	0.20
8	-0.10 ± 0.07	0.13	-0.19 ± 0.05	0.20	-0.12 ± 0.08	0.14	-0.16 ± 0.15	0.22

ORCID iDs

Bingfei Fan https://orcid.org/0000-0002-9531-3549
Tao Liu https://orcid.org/0000-0002-2797-0264

References

[1] Tao W, Liu T, Zheng R and Feng H 2012 Gait analysis using wearable sensors *Sensors* **12** 2255–83
[2] Alcock L, Galna B, Lord S and Rochester L 2016 Characterisation of foot clearance during gait in people with early Parkinson's disease: deficits associated with a dual task *J. Biomech.* **49** 2763–9
[3] Pirker W and Katzenschlager R 2017 Gait disorders in adults and the elderly: a clinical guide *Wien. Klin. Wochenschr.* **129** 81–95
[4] Lai D T H, Taylor S B and Begg R K 2012 Prediction of foot clearance parameters as a precursor to forecasting the risk of tripping and falling *Hum. Mov. Sci.* **31** 271–83
[5] Schulz B W 2017 A new measure of trip risk integrating minimum foot clearance and dynamic stability across the swing phase of gait *J. Biomech.* **55** 107–12
[6] Pfortmueller C A, Lindner G and Exadaktylos A K 2014 Reducing fall risk in the elderly: risk factors and fall prevention, a systematic review *Minerva Med.* **105** 275–81
[7] Kearney F C, Harwood R H, Gladman J R F, Lincoln N and Masud T 2013 The relationship between executive function and falls and gait abnormalities in older adults: a systematic review *Dement. Geriatr. Cogn. Disord.* **36** 20–35
[8] Lu T, Chen S and Chiu H 2012 Best-compromise between mechanical energy expenditure and foot clearance predicts leading limb motion during obstacle-crossing *Gait Posture* **36** 552–6
[9] Telonio A, Blanchet S, Maganaris C N, Baltzopoulos V and McFadyen B J 2013 The detailed measurement of foot clearance by young adults during stair descent *J. Biomech.* **46** 1400–2
[10] Begg R, Best R, Dell'Oro L and Taylor S 2007 Minimum foot clearance during walking: strategies for the minimisation of trip-related falls *Gait Posture* **25** 191–8

[11] Graci V, Elliott D B and Buckley J G 2009 Peripheral visual cues affect minimum-foot-clearance during overground locomotion *Gait Posture* **30** 370–4
[12] Mariani B, Hoskovec C, Rochat S, Buela C, Penders J and Aminian K 2010 3D gait assessment in young and elderly subjects using foot-worn inertial sensors *J. Biomech.* **43** 2999–3006
[13] Mariani B, Rochat S, Buela C J and Aminian K 2012 Heel and toe clearance estimation for gait analysis using wireless inertial sensors *IEEE Trans. Biomed. Eng.* **59** 3162–8
[14] Kitagawa N and Ogihara N 2016 Estimation of foot trajectory during human walking by a wearable inertial measurement unit mounted to the foot *Gait Posture* **45** 110–4
[15] McGrath D, Greene B R, Walsh C and Caulfield B 2011 Estimation of minimum ground clearance (MGC) using body-worn inertial sensors *J. Biomech.* **44** 1083–8
[16] Yun X P, Calusdian J, Bachmann E R and McGhee R B 2012 Estimation of human foot motion during normal walking using inertial and magnetic sensor measurements *IEEE Trans. Instrum. Meas.* **61** 2059–72
[17] Hannink J, Ollenschlaeger M, Kluge F, Roth N, Klucken J and Eskofier B M 2017 Benchmarking foot trajectory estimation methods for mobile gait analysis *Sensors* **17** 1940
[18] Arami A, Saint Raymond N and Aminian K 2017 An accurate wearable foot clearance estimation system: toward a real-time measurement system *IEEE Sens. J.* **17** 2542–9
[19] Kanzler C M, Barth J, Rampp A, Schlarb H, Rott F, Klucken J and Eskofier B M 2015 Inertial sensor based and shoe size independent gait analysis including heel and toe clearance estimation *37th Annual Int. Conf. IEEE Engineering in Medicine and Biology* Society *(EMBC)* (*Milan, Italy*) pp 5424–7
[20] Mills P M, Barrett R S and Morrison S 2008 Toe clearance variability during walking in young and elderly men *Gait Posture* **28** 101–7
[21] Qiu S, Wang Z, Zhao H, Liu L, Li J, Jiang Y and Fortino G 2019 Body sensor network-based robust gait analysis: toward clinical and at home use *IEEE Sens. J.* **19** 8393–401
[22] Santhiranayagam B K, Lai D T H, Sparrow W A and Begg R K 2015 A machine learning approach to estimate minimum toe clearance using inertial measurement units *J. Biomech.* **48** 4309–16
[23] Pham Duy D and Suh Y S 2015 Foot pose estimation using an inertial sensor unit and two distance sensors *Sensors* **15** 15888–902
[24] Wahab Y, Bakar N A and Mazalan M 2014 Error correction for foot clearance in real-time measurement. *Int. Conf. on Science and Engineering in Mathematics, Chemistry and Physics (ScieTech)* (*Jakarta, Indonesia*) vol 495
[25] Fan B, Li Q and Liu T 2018 Improving the accuracy of wearable sensor orientation using a two-step complementary filter with state machine-based adaptive strategy *Meas. Sci. Technol.* **29** 115104
[26] Madgwick S 2014 AHRS algorithms and calibration solutions to facilitate new applications using low-cost MEMS *PhD Thesis* University of Bristol, Bristol, UK
[27] Fan B, Li Q and Liu T 2018 How magnetic disturbance influences the attitude and heading in magnetic and inertial sensor-based orientation estimation *Sensors* **18** 76
[28] Yun X, Bachmann E R, Moore H and Calusdian J 2007 Self-contained position tracking of human movement using small inertial/magnetic sensor modules *IEEE Int. Conf. on Robotics and Automation* (Rome, Italy) p 2526
[29] Skog I, Handel P, Nilsson J-O and Rantakokko J 2010 Zero-velocity detection—an algorithm evaluation *IEEE Trans. Biomed. Eng.* **57** 2657–66
[30] Li Q, Young M, Naing V and Donelan J M 2010 Walking speed estimation using a shank-mounted inertial measurement unit *J. Biomech.* **43** 1640–3
[31] Dadashi F, Mariani B, Rochat S, Buela C J, Santos-Eggimann B and Aminian K 2014 Gait and foot clearance parameters obtained using shoe-worn inertial sensors in a large-population sample of older adults *Sensors* **14** 443–57